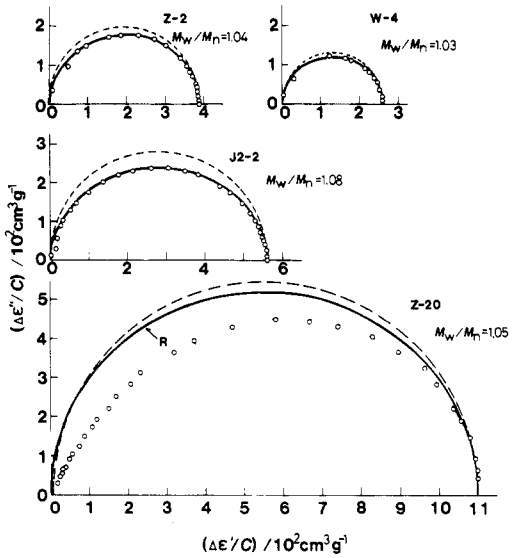


**Figure 12.** Cole–Cole plots for PHIC fractions in toluene at 25 °C. Circles, experimental data; dashed semicircles, Debye curves; thick solid curves, theoretical curves calculated by eq 9 and 10 for the indicated values of $M_w/M_n$ (see text).

above the data points. This shows that the dispersion is still polydisperse in relaxation time even after being corrected for the sample's polydispersity. The polydispersity was found to set in at $M_w$ of about 70 000 and become remarkable with increasing molecular weight. Yoshizaki and Yamakawa[11] have predicted a deviation which originates from internal modes of motion of the chain, but it is considerably smaller than that observed here. This invites a further theoretical investigation of this problem.

**Acknowledgment.** We thank Dr. Takashi Norisuye for stimulating discussions. This work was in part supported by the Institute for Macromolecular Research, Osaka University.

**Registry No.** PHIC, 26746-07-6.

## References and Notes

(1) Bur, A. J.; Fetters, L. J. *Chem. Rev.* **1977**, *76*, 727.
(2) Bur, A. J.; Roberts, D. E. *J. Chem. Phys.* **1969**, *51*, 406.
(3) Bur, A. J. *J. Chem. Phys.* **1970**, *52*, 3813.
(4) Fetters, L. J.; Yu, H. *Macromolecules* **1971**, *4*, 385.
(5) Berger, M. N.; Tidswell, B. M. *J. Polym. Sci., Polym. Symp.* **1973**, *42*, 1063.
(6) Murakami, H.; Norisuye, T.; Fujita, H. *Macromolecules* **1980**, *13*, 345.
(7) Kuwata, H.; Murakami, H.; Norisuye, T.; Fujita, H. *Macromolecules* **1984**, *17*, 2731.
(8) Itou, T.; Chikiri, H.; Teramoto, A. *Polym. J.* **1988**, *20*, 143.
(9) Lochhead, R. Y.; North, A. M. *Trans. Faraday Soc.* **1972**, *68*, 1089.
(10) Anderson, J. S.; Vaughan, W. E. *Macromolecules* **1975**, *8*, 454.
(11) Yoshizaki, T.; Yamakawa, H. *J. Chem. Phys.* **1984**, *81*, 982.
(12) Conio, G.; Bianchi, E.; Ciferri, A.; Krigbaum, W. R. *Macromolecules* **1984**, *17*, 2731.
(13) Shashoua, V. E.; Sweeny, W.; Tietz, R. F. *J. Am. Chem. Soc.* **1960**, *82*, 866.
(14) Aharoni, S. M. *Macromolecules* **1979**, *12*, 94.
(15) Matsumoto, T.; Nishioka, N.; Teramoto, A.; Fujita, H. *Macromolecules* **1974**, *7*, 824.
(16) Stockmayer, W. H. *Pure Appl. Chem.* **1967**, *15*, 539.
(17) Wada, A. J. *Chem. Phys.* **1959**, *31*, 495; *Bull. Chem. Soc. Jpn.* **1960**, *33*, 822.
(18) Applequist, J.; Mahr, T. G. *J. Am. Chem. Soc.* **1966**, *88*, 5419.
(19) Buckingham, A. D. *Aust. J. Chem.* **1952**, *6*, 93, 323.

# Excluded-Volume Effects in Rubber Elasticity. 4. Nonhydrostatic Contribution to Stress

**J. Gao and J. H. Weiner***

*Department of Physics and Division of Engineering, Brown University, Providence, Rhode Island 02912.* *Received May 11, 1988*

ABSTRACT: Molecular dynamics simulations of idealized network models demonstrate that the noncovalent excluded-volume (EV) interaction makes a significant nonhydrostatic contribution to the stress tensor when $\phi$, the fraction of occupied volume, is above ~0.3. This contribution grows with $\phi$ and, at the same time, the covalent contribution decreases. As a result, the noncovalent EV interaction rapidly becomes the dominant source of deviatoric stress in the network. The simulations show that the covalent bonds introduce directional screening of the noncovalent EV interaction; this provides the mechanism with its nonhydrostatic contribution. They also show that the average force in the covalent bonds decreases with increase in $\phi$; this is the reason for the decrease in the covalent contribution.

## 1. Introduction

We continue in this paper our investigations into the role of excluded volume (EV) in rubber elasticity. As in the previous papers of this series,[1-3] our principal tool is the computer simulation of idealized atomic systems. Our hope is that the study of these systems may provide insight into the details of the mechanisms of atomic interactions, both covalent and noncovalent; the resulting physical picture can then be compared with those underlying the various molecular theories that have been but forward for rubberlike solids.

We have begun our studies with highly idealized systems for two reasons. The first is the practical one, that computer time requirements go up rapidly with increased realism of the model. This makes difficult extensive studies, including the effects of wide parameter variation. The second reason for starting with simple models is that it is easier to grasp the essential features of what is going on when they are employed. When the significant features of the behavior of the idealized models become clear, we plan to use them as a guide for the study of more realistic models and to determine to what extent the observations on the idealized models carry over.

Of principal concern in these studies has been the nature of the contribution of the noncovalent EV interaction to the stress. In our previous work, where the simulations were restricted to systems with relatively small occupied volume fractions, we found that the EV contribution to

0024-9297/89/2222-0979$01.50/0 

the stress tensor was purely hydrostatic but that, nevertheless, the noncovalent EV potential had important indirect effects on the stress tensor. In this paper, we consider simulations of systems with larger occupied volume fraction, and we will see that then there are significant direct EV contributions to the deviatoric stress as well.

**Chain Model.** In the spirit of using idealized systems, we continue to employ the simplest chain model that has both the covalent bonding characteristic of macromolecules and the attribute of excluded volume. It approximates the hard-sphere, freely jointed chain. For computational and conceptual convenience the covalent potential is represented by a stiff linear spring and the hard-sphere potential is replaced by the repulsive part of the Lennard-Jones potential. That is, the covalent potential $u_c(r)$ is

$$u_c(r) = \tfrac{1}{2}\kappa(r - a)^2 \tag{1.1}$$

where $r$ is the distance between adjacent atoms on a given chain and the noncovalent potential is

$$\begin{aligned} u_{nc}(r) &= 4\epsilon[(\sigma/r)^{12} - (\sigma/r)^6] \quad \text{for} \quad r \leqslant r_0 \\ &= u_{nc}(r_0) \quad \text{for} \quad r \geqslant r_0 \end{aligned} \tag{1.2}$$

where $r$ denotes the distance between any adjacent pair of atoms on a given chain or between any pair of atoms on different chains and $r_0 = 2^{1/6}\sigma$. The results reported in this paper were all carried out for $\sigma = a$, $\kappa a^2/kT = 202$, and $\epsilon/kT = 0.5$. For these parameter values, the bond length undergoes only small fractional changes and $\sigma$ may be regarded as an effective hard-sphere diameter.[4] It should be noted that in this model the temperature-independent potential $u_c(r)$ of eq 1.1 represents a single covalent bond and not a Gaussian chain as in the Rouse model.

**Reduced Density.** In view of the close relation of $\sigma$ to a hard-sphere diameter, we defined the reduced density $\rho$ of the system as

$$\rho = n\sigma^3/v \tag{1.3}$$

where $n$ is the number of atoms in volume $v$. In our previous work,[2,3] we employed network models in which the chain end-to-end vector was tied to the dimensions of the basic cell employed in conjunction with periodic boundary conditions. As a result, the maximum density studied was $\rho = 0.388$. (Note that the fraction of occupied volume by a system of nonintersecting spheres of diameter $\sigma$ is $(\pi/6)\rho$.) It is the purpose of the present paper to consider models that permit us to study larger values of $\rho$.

**Virial Stress Formula.** The state of stress for a system of such chains consisting of a total of $n$ atoms in volume $v$ at temperature $T$ is given by the generalized virial stress formula[5] as

$$vt_{ij} = -nkT\delta_{ij} + \sum_{\alpha} \langle r_\alpha^{-1} u'_\alpha(r_\alpha) y_i(\alpha) y_j(\alpha) \rangle \tag{1.4}$$

where $t_{ij}$, $i, j = 1, 2, 3$, are the components of the stress tensor, force per unit area in the deformed system, referred to a rectangular Cartesian coordinate system $x_i$, $\delta_{ij}$ is the Kronecker delta; $\alpha$ ranges over all pairs of atoms; $\mathbf{r}_\alpha$ is the vector displacement between the $\alpha$ pair, $r_\alpha = |\mathbf{r}_\alpha|$; $u'_\alpha(r_\alpha)$ is the derivative of the potential for this pair; $y_i(\alpha)$ are the components of $\mathbf{r}_\alpha$ with respect to the coordinate system $x_i$; and brackets denote long-time averages. We may also rewrite eq 1.4, to make the two types of interactions $u_c$ and $u_{nc}$ explicit, as

$$\begin{aligned} vt_{ij} = -nkT\delta_{ij} &+ \sum_{\alpha\epsilon c} \langle r_\alpha^{-1} u'_c(r_\alpha) y_i(\alpha) y_j(\alpha) \rangle + \\ &\sum_{\alpha\epsilon nc} \langle r_\alpha^{-1} u'_{nc}(r_\alpha) y_i(\alpha) y_j(\alpha) \rangle \end{aligned} \tag{1.5}$$

where the notations $\alpha \epsilon$ c or $\alpha \epsilon$ nc indicate that the sums range over all pairs of covalently or noncovalently interacting atoms, respectively.

**Mean and Deviatoric Stress.** It is found experimentally that rubberlike materials undergoing deformations such as uniaxial extension do so with negligible change of volume, and most theories idealize these deformations as constant volume. It then follows[6] that these theories do not determine the full stress tensor as a function of the parameters describing the deformation but leave the mean stress (or its negative, the pressure) to be determined from the boundary conditions. It is convenient, therefore, to express the stress tensor $t_{ij}$ as a sum of an isotropic pressure $p$ and a deviatoric stress $\tau_{ij}$ by the relations

$$t_{ij} = \tau_{ij} - \delta_{ij}p \tag{1.6}$$

where

$$p = -\tfrac{1}{3}\sum_{i=1}^{3} t_{ii} \tag{1.7}$$

In terms of the virial stress expression of eq 1.4, we can express the pressure $p$ and the deviatoric stress $\tau_{ij}$ as

$$pv = nkT - \tfrac{1}{3}\sum_{\alpha\epsilon c} \langle r_\alpha u'_c(r_\alpha) \rangle - \tfrac{1}{3}\sum_{\alpha\epsilon nc} \langle r_\alpha u'_{nc}(r_\alpha) \rangle \tag{1.8}$$

and

$$\tau_{ij}v = \tfrac{2}{3}\sum_{\alpha\epsilon c} \langle r_\alpha u'_c(r_\alpha) Y_{ij}(\alpha) \rangle + \tfrac{2}{3}\sum_{\alpha\epsilon nc} \langle r_\alpha u'_{nc}(r_\alpha) Y_{ij}(\alpha) \rangle = \tau_{ij}^{c}v + \tau_{ij}^{nc}v \tag{1.9}$$

where $\tau_{ij}^{c}$ and $\tau_{ij}^{nc}$ are respectively the covalent and noncovalent contributions to the deviatoric stress and where the quantities

$$Y_{ij}(\alpha) = \tfrac{1}{2}\left[\frac{3y_i(\alpha)y_i(\alpha)}{r_\alpha^2} - \delta_{ij}\right] \tag{1.10}$$

are measures of the orientation of $\mathbf{r}_\alpha$, the vector connecting the $\alpha$ pair of interacting atoms; in particular, if $\mathbf{e}_\alpha = \mathbf{r}_\alpha/r_\alpha$ is uniformly distributed on the unit sphere, then $\langle Y_{ij}(\alpha) \rangle \equiv 0$.

**Bond Force.** The virial stress formula, in the various forms presented above, contains as an important component the covalent bond force $\hat{f}_b^{c} = u'_c(r_\alpha)$. (We use the notation $f_b^{c} = \langle \hat{f}_b^{c} \rangle = \langle u'_c(r_\alpha) \rangle$ for the time average of this fluctuating quantity.) In this sense, the virial formula gives a more local view of the stress in a macromolecular system than the usual entropic view, in which the significant force is the axial force acting on the chain.

The distinction between these two forces has been stressed by Weiner and Berman[7] who treated the ideal, freely jointed chain (i.e., $\sigma = 0$, in the terminology of eq 1.1 and 1.2). For this case, they found that $f_b^{c} = 2kT/a$ when the end-to-end vector of the chain is zero and the axial force vanishes. This nonzero value of $f_b^{c}$ may be understood in terms of the centrifugal force acting in a bond connecting two atoms in thermal motion. A heuristic derivation can be given by considering a single atom in thermal motion connected by a covalent bond of length $a$ to a fixed point (Figure 1). Then $\hat{f}_b^{c} = mv^2/a$, where $v$ is the instantaneous atomic velocity and $\langle mv^2 \rangle = 2kT$ since the atom has two degrees of freedom.

We have begun the study of the effect of EV interactions on $f_b^{c}$ in our earlier work.[2] There it was found that $f_b^{c}$ is nearly constant for small values of $R/Na$, where $R$ is the end-to-end distance and $Na$ is the fully extended length of the chain, and the following discussion is confined to this regime. At low values of $\rho$, where intrachain EV

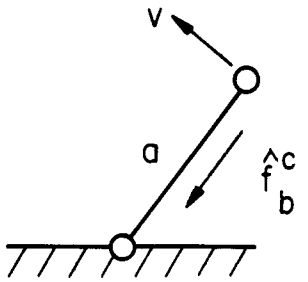


**Figure 1.** Heuristic model for centrifugal force as contributor to covalent bond force.

dominates, its effect is to cause a relatively small increase in $f_b^c$ over its ideal value. However, as $\rho$ increases and interchain EV becomes more important, $f_b^c$ decreases. In this paper we carry the study of the dependence of $f_b^c$ on $\rho$ to regimes of higher density.

**van der Waals Picture.** As in our previous work, we continue to adopt the viewpoint known in the theory of liquids as the van der Waals picture,[8] which states that it is the strongly repulsive part of the noncovalent potential that, together with the covalent bonds, plays the primary role in determining the structure of the system. The attractive portion of the noncovalent potential may be regarded in first approximation as "a spatially uniform background potential which .. merely provides the cohesive energy that makes the system stable at a particular density and pressure".[8] Therefore, we take the reduced density, $\rho$, eq 1.3, as an independent parameter, with the variation in behavior of the system with $\rho$ as the question of particular interest. We are assuming that the addition of an attractive tail to $u_{nc}$ will primarily affect the value of the pressure $p$ corresponding to a given $\rho$ and $T$ but will leave the deviatoric stress $\tau_{ij}$ and the bond force $f_b^c$ substantially unchanged. As noted previously, when dealing with those deformations, such as uniaxial extension, for which the assumption of constant volume is appropriate, it is only the deviatoric stress $\tau_{ij}$ which is of interest in any case since the pressure is determined by the boundary conditions, e.g., by the condition that the transverse surfaces are free of stress in uniaxial extension. Furthermore, the observed entropic character of the deviatoric stress in such deformations leads to the conclusion that EV and packing effects play a primary role in determining its value.[9,10]

The outline of the remainder of the paper is as follows: In section 2, the molecular dynamics of a polymer melt is described, with principal emphasis of the behavior of the bond force as a function of melt density. The insights gained from consideration of the melt are then applied to the simulation of a network in section 3. Conclusions and a summary of results are contained in section 4.

## 2. Melt Simulation

In this section we discuss the simulation by molecular dynamics of a canonical ensemble (temperature $T$) of a melt of $\nu$ chains, each with $N$ bonds, with periodic boundary conditions employed to remove surface effects (Figure 2). The basic cell has volume $v$ so that $\rho = n\sigma^3/v$ with $n = \nu(N + 1)$. Details of the calculation procedure are given in the Appendix.

It is clear that the deviatoric stress $\tau_{ij}$ should vanish identically for the melt in a uniform equilibrium state since there is then no preferred direction in the melt. However, as seen in previous calculations made in connection with the work of ref 2, $f_b^c = \langle u'_c(r_\alpha)\rangle$ is nonzero in the melt and, indeed, depends upon $\rho$ in much the same way for both network and melt. Therefore, one of the principal questions to be studied through the melt simulations is the

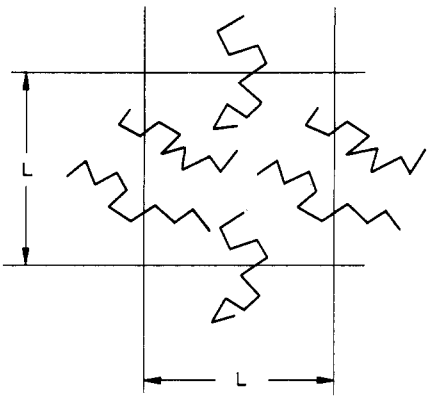


**Figure 2.** Schematic illustration of periodic boundary conditions for molecular dynamics simulation of a polymer melt.

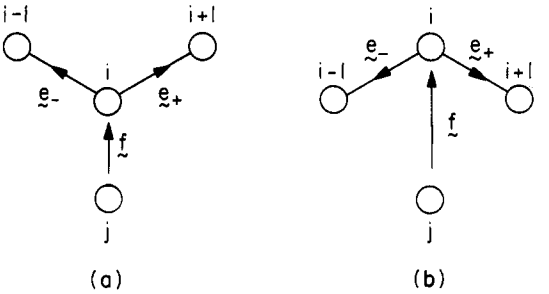


**Figure 3.** Directional screening of the EV interaction (force **f**) between atoms $j$ and $i$ by atoms $i - 1$ and $i + 1$, which are covalently bonded to $i$. EV interaction between $j$ and $i$ occurs more frequently when atoms $i - 1$, $i$, and $i + 1$ are in a convex configuration (a) than when they are in a concave configuration (b).

dependence of $f_b^c$ upon $\rho$, extending the previous results to the higher density regime.

Another question that we wish to study by means of the melt simulation is the extent to which the covalently bonded chain structure imposes a preferred directionality on the noncovalent EV interaction. While it is true that in the melt $\langle Y_{ij}(\alpha)\rangle \equiv 0$ for a pair in noncovalent interaction, this states only that this interaction direction is random with respect to a fixed laboratory frame. It is nevertheless possible that certain directions relative to the instantaneous chain configuration are favored for noncovalent interaction.

To examine the latter possibility, we introduce the following notation: Consider three successive atoms $i - 1$, $i$, and $i + 1$ along a given chain and atom $i$ subjected at a given instant to the noncovalent repulsive force **f** exerted by atom $j$ (Figure 3). Let $\mathbf{e}_+$ and $\mathbf{e}_-$ be the unit vectors along the bonds from $i$ to $i + 1$ and $i - 1$, respectively, and define

$$\hat{f}_b^{nc}(i) = \tfrac{1}{2}(\mathbf{f}\cdot\mathbf{e}_+ + \mathbf{f}\cdot\mathbf{e}_-) \qquad (2.1)$$

and $f_b^{nc}$ is the time average of $\hat{f}_b^{nc}(i)$ averaged over all of the atoms of the system. (For the end atoms of the chain, the term corresponding to $\mathbf{e}_+$ or $\mathbf{e}_-$ is omitted.)

It may be seen that if the configuration $i - 1$, $i$, $i + 1$ is convex to the direction $j$, $i$ as in Figure 3a, then $\hat{f}_b^{nc}(i) > 0$; i.e., the force exerted on $i$ is in the same direction as that which would be exerted by tensile covalent bond forces, $f_b^c > 0$. On the other hand, if the configuration $i - 1$, $i$, $i + 1$ is concave with respect to $j$, $i$, as in Figure 3b, then $\hat{f}_b^{nc}(i) < 0$. If, therefore, the directions of noncovalent interactions are insensitive with respect to chain configurations we would expect that $f_b^{nc} = 0$.

Results of simulations carried out for a system of 10 chains per cell, each with 20 bonds, are shown in Figure 4 for various values of $\rho$. It is seen that (1) the covalent

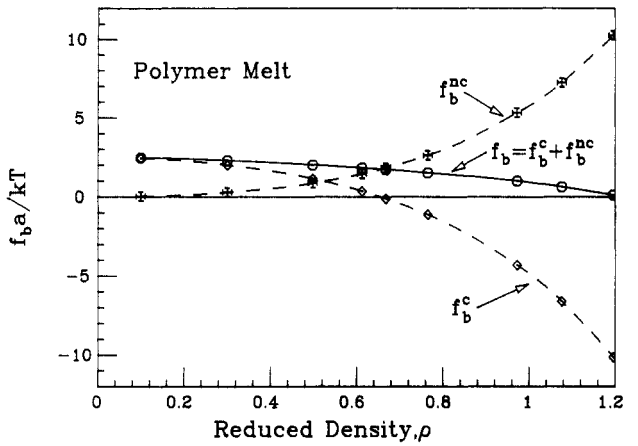


**Figure 4.** Dependence of forces in bond directions in the melt on reduced density $\rho$. $f_b^c$ is the average force in the covalent bonds, $f_b^{nc}$ is the average component of the noncovalent EV interaction force taken in the bond direction (eq 2.1), and $f_b$ is their sum. The melt has 10 chains per cell, each with 20 bonds.

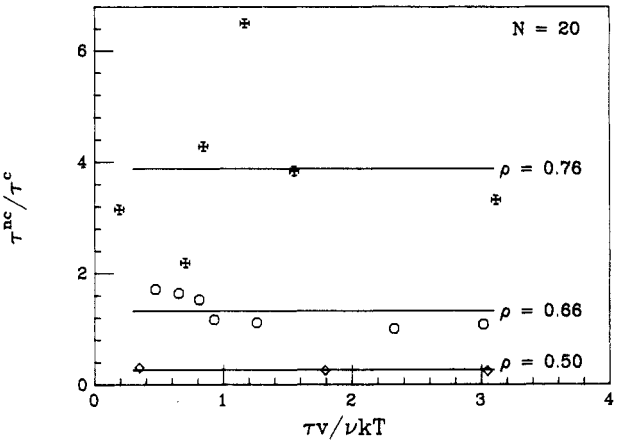


**Figure 5.** Value of ratio $\tau^{nc}/\tau^c$ (see eq 3.1) for network models with different reduced densities $\rho$. For each density, the horizontal line shown is the average of all values of $\tau^{nc}/\tau^c$ for that density. The network has 24 chains per cell, each with 20 bonds.

bond force, $f_b^c$, decreases with increasing $\rho$ and, in fact, becomes negative at sufficiently high densities; (2) the noncovalent bond force, $f_b^{nc}$, is zero for $\rho = 0$ and increases monotonically with $\rho$; and (3) the sum $f_b = f_b^c + f_b^{nc}$ is positive for small $\rho$ and decreases monotonically with $\rho$. (Preliminary simulations at larger values of $\rho$ indicate that $f_b$ becomes negative at $\rho \sim 1.2$ and that a transition analogous to the fluid–solid transition observed in the hard-sphere system[11] occurs in that vicinity; we reserve detailed investigation of this possibility for future work.)

From the fact that $f_b^{nc} > 0$ we may conclude, as discussed above, that noncovalent repulsive interactions occur more frequently in the convex chain configuration (Figure 3a) than in the concave (Figure 3b); this may be understood as a consequence of the selective screening effect of the atoms $i-1$, $i+1$, inhibiting the $j$, $i$ interaction when they are in the latter configuration. We may expect this screening action to have important consequences in a network and we study this question in the following section.

## 3. Network Simulation

The results of the melt simulations described in the previous section have important implications for the change with increasing $\rho$ of the relative values of $\tau_{ij}^c$ and $\tau_{ij}^{nc}$, the covalent and noncovalent contributions to the deviatoric stress, eq 1.9.

(1) The decrease of $f_b^c = \langle u'_c \rangle$ with $\rho$ suggests that there may be a corresponding decrease in $\tau_{ij}^c$ although, as seen from eq 1.9, $\tau_{ij}^c$ and $\langle u'_c \rangle$ need not be directly proportional.

(2) As far as the noncovalent interactions are concerned, it was seen in the melt that screening introduces preferred directions for repulsive EV interactions relative to instantaneous bond orientations, and this effect becomes increasingly important with increase in $\rho$. In a network, bond directions have, on average, preferred orientations in space, and therefore the same should be the case for the directions of EV interactions. This suggests (eq 1.9) that $\tau_{ij}^{nc}$ should increase with $\rho$.

We describe tests of these hypotheses in this section, made by the simulation of a model network. As far as the questions at hand are concerned, the critical distinction between a melt and a network is that in the melt $\langle \mathbf{R} \rangle = 0$, where $\mathbf{R}(t)$ is the end-to-end vector of an arbitrary chain of the system, while in the network $\langle \mathbf{R} \rangle \neq 0$.[12] To create a model network, therefore, we start with a melt in thermal equilibrium and, at an arbitrary instant of time, stop the motion of the end atoms of all of the chains, while the thermal motion of all of the other atoms continues as before. The model network thus formed differs from real networks in at least two ways; the chain vectors, $\mathbf{R}$, are strict constants and do not fluctuate and the chains are not interconnected at junction points. Nevertheless the model serves to evaluate the particular question we are concerned with here: the change in relative importance of $\tau_{ij}^c$ and $\tau_{ij}^{nc}$ as $\rho$ increases.

The basic cell size employed in the simulations in conjunction with periodic boundary conditions is relatively small; typically it is a cube with edge $L \cong 9a$, or $L \sim 13.5$ Å. Therefore, the procedure of suddenly arresting the end-to-end vectors of the molecules of the melt at an arbitrary instant does not lead to a state with zero deviatoric stress, as would be expected for much larger values of $L$. This means that the deviatoric stress $\tau_{ij}$ in the network which is obtained by the virial formula by time averaging over a suitable period after it has been formed is not subject to direct control in this computation. In order to obtain a scalar measure $\tau$ of the deviatoric stress state, the square root of the second invariant of the tensor $\tau_{ij}$ was employed, that is

$$\tau = (\tfrac{1}{2} \sum_{i,j=1}^{3} \tau_{ij}\tau_{ij})^{1/2} \tag{3.1}$$

where we will refer to $\tau$ as the effective shear stress, with corresponding definitions for $\tau^c$ and $\tau^{nc}$ based on $\tau_{ij}^c$ and $\tau_{ij}^{nc}$, respectively.

As noted previously, the value of $\tau$ corresponding to the network obtained by fixing end-to-end vectors in a melt at an abrbitrary instant is not subject to direct control. In order to produce networks corresponding to a wider range of $\tau$, in some cases the end atoms of the chains in the as-formed network were caused to move further under the action of an applied force pair which tended to increase the end-to-end chain distance. This procedure was followed for a limited period, the end atoms were again fixed, and the deformed network was allowed to equilibrate.

The results for the ratios of $\tau^{nc}/\tau^c$ as a function of $\tau$ are shown in Figures 5 and 6. There is considerable scatter in the computed values of this ratio at the highest density, $\rho = 0.76$, studied in this connection. This appears to be due to the larger relaxation times at this density. Nevertheless, it is clear from the simulation results that $\tau^{nc}/\tau^c$ depends very strongly upon $\rho$. For $\rho < 0.4$, this ratio is essentially zero, as observed in our previous simulations. However, for $\rho > 0.5$, $\tau^{nc}/\tau^c$ grows very rapidly with $\rho$, reaching values of $\tau^{nc}/\tau^c \sim 4$ for $\rho \sim 0.8$.

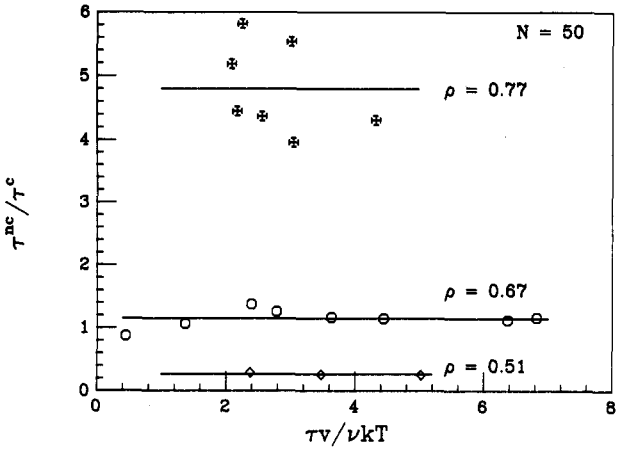


**Figure 6.** Same as Figure 5, but the network has 10 chains per cell, each with 50 bonds.

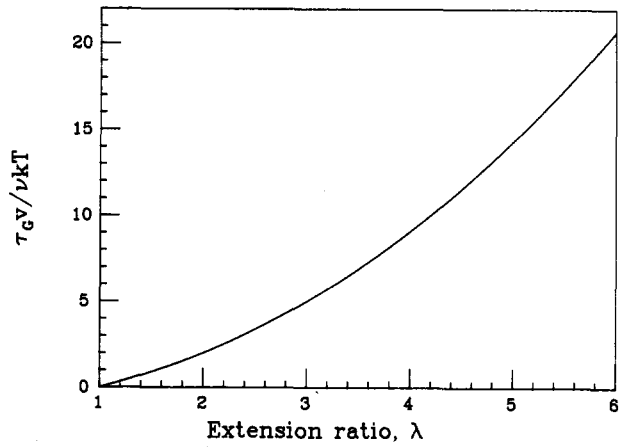


**Figure 7.** Effective shear stress, $\tau_G$, for the three-chain model (so that $\nu = 3$ in this case) with Gaussian chains in uniaxial extension $\lambda$.

To aid in interpreting the range of values of $\tau$ shown in Figures 5 and 6, we may utilize the effective shear stress $\tau_G$ obtained on the basis of the familiar three-chain model employing Gaussian chains for a body undergoing a uniaxial extension $\lambda$:

$$\tau_G = \frac{3^{1/2}}{\upsilon} kT|\lambda^2 - \lambda^{-1}| \qquad (3.2)$$

This relation is shown in Figure 7, which may be used to obtain an estimate of the extension ratio $\lambda$ corresponding to a particular value of $\tau$. From this graph, we see that the range of $\tau$ covered in Figure 5 is roughly equivalent to an extension range of $1 < \lambda < 2.5$ in an ideal Gaussian network, while that covered in Figure 6 corresponds to $1 < \lambda < 3.5$.

## 4. Conclusions

The physical picture of the nature of stress in rubberlike solids that emerges from our computer simulations of an idealized model is strikingly different from the usual ones. Beginning with the classical molecular theories, which had their origins over 50 years ago, the concept of the chain in tension acting as an entropic spring has played a central role. The concept of excluded volume was invoked in these theories only to explain why such a system of chains did not collapse to a point. The effect of the repulsive EV potential was assumed to be the contribution of a purely hydrostatic pressure to the stress tensor which counterbalanced the tension in the chains. Furthermore, the assumption that deformations such as uniaxial extension take place at constant volume meant that the pressure in the system was determined by the stress boundary conditions and, therefore, did not have to be explicitly treated by a molecular theory.

The earliest molecular theories have been described by Flory as utilizing phantom networks, since they completely neglected chain–chain interactions and permitted chains to pass through one another. Spurred by discrepancies between such theories and experiment as demonstrated, for example, by Mooney-Rivlin plots for uniaxial tension experiments,[13] many theories have been put forward to include some of the interactions neglected in the phantom network. Some introduce noncovalent interactions through their effect on cross-link fluctuations,[14-17] as confining tubes[18-23] or entangling slip-links.[24] However, the role of the chain as an entropic spring in tension remains central to these theories.

In order to reexamine this physical picture, we have considered in this paper idealized polymer systems in which the chains are freely jointed with the covalent bonds represented by stiff linear springs, and the repulsive EV potential closely approximates a hard-sphere potential, with $\sigma$ the hard-sphere diameter. A key parameter characterizing these systems is the reduced density $\rho = n\sigma^3/\upsilon$, where $n$ is the number of atoms in volume $\upsilon$ or, equivalently, $\phi = (\pi/6)\rho$, where $\phi$ is the fraction of volume occupied by the hard spheres.

The molecular dynamics simulations of these model systems have been interpreted on the basis of the virial stress formula.[5] This formula focuses on the forces in the covalent bonds and therefore gives a more local view of stress in rubberlike systems than the usual chain view. Of particular interest, therefore, is $f_b^c$, the mean force in a covalent bond of the system. In the absence of EV, i.e., for $\sigma = 0$, $f_b^c > 0$, denoting a tensile force in the bond and in correspondence to the tensile axial force exerted by an ideal chain. The covalent bond force $f_b^c$ for an isolated chain with EV continues to be tensile. However, as the reduced density $\rho$, or the volume fraction $\phi$, increases for a system of interacting chains, it is found that $f_b^c$ decreases[25] and becomes negative at values of $\phi \cong 0.3$. Therefore, the usual physical picture of the chains transmitting tensile forces through their covalent bonds does not apply to these model systems.

With the covalent bonds in compression, one may then ask how such a system can produce tensile stresses in response to uniaxial extension. The answer is provided, in part, by the examination of the results of the molecular dynamics simulation of a system of the model chains corresponding to a melt. The time average of the components of the repulsive EV interactions taken in the chain bond directions are denoted by $f_b^{nc}$ (see eq 2.1 et seq.). If the spherically symmetric repulsive EV interactions took place independently of the covalent interactions, then clearly one would find $f_b^{nc} = 0$. Instead, what is found is that $f_b^{nc} > 0$, indicating that the two types of interactions are correlated. Furthermore, the fact that $f_b^{nc}$ is always positive (i.e., tensile in character) shows that the correlation may be attributed to screening, Figure 3. It is also found that, in the range of $\rho$ to be expected in rubberlike solids, the increase of $f_b^{nc}$ with $\rho$ compensates in part the decrease of $f_b^c$, so that $f_b = f_b^c + f_b^{nc} > 0$; however, $f_b$ decreases monotonically with $\rho$ and eventually changes sign at $\rho = 1.2$ (or at $\phi \cong 0.6$).

Bond orientations in the melt are randomly distributed in space, so the fact that $f_b$ is positive does not give rise to any deviatoric stress in that system. To study the relative covalent and noncovalent contributions to the deviatoric stress, we next considered a model network

constructed from the molecular dynamics simulation of a melt by suddenly fixing the end-to-end vectors of each chain by fixing their end atoms, while the other atoms continue in thermal motion. The deviatoric stress, $\tau_{ij}$, in these randomly created networks was computed by means of the viral stress formula, eq 1.9, and $\tau = (^1/_2\tau_{ij}\tau_{ij})^{1/2}$, summation convention, was used as a scalar measure of the deviatoric stress. Also computed were the covalent and noncovalent contributions to the deviatoric stress, $\tau_{ij}^{c}$ and $\tau_{ij}^{nc}$, eq 1.9, and the corresponding measures $\tau^{c}$ and $\tau^{nc}$. It was found that $\tau^{nc}/\tau^{c}$ was essentially zero for $\rho < 0.5$. This is in agreement with the previous simulation results for the three-chain model of ref 2, which was restricted to values of $\rho < 0.4$. However, as $\rho$ increases beyond 0.5, the ratio $\tau^{nc}/\tau^{c}$ grows rapidly, with values of $\tau^{nc}/\tau^{c} \sim 4$ for $\rho \sim 0.8$.

We have therefore been led to a physical picture of stress in rubberlike solids which is in substantial contradiction to the usual one. Instead of the covalent and noncovalent EV systems being decoupled, we find that there is a close coupling between the two. This coupling is due to the directional screening of EV interactions by atomic groups whose mutual orientation is determined by the covalent bonds. A consequence of this coupling is that there is a substantial noncovalent contribution to the deviatoric stress and this contribution becomes the overwhelmingly dominant one at values of density beyond $\rho \sim 0.8$ (or volume fractions beyond $\phi \sim 0.4$).

We have arrived at this picture on the basis of the simulations of a highly idealized model. Nevertheless, it appears to us quite likely that similar mechanisms should apply as well to more realistic systems. One of the most severe idealizations in our present model is the use of freely jointed chains, and we plan soon to extend these studies to chains with valence angle restrictions.

**Acknowledgment.** This work has been supported by the Gas Research Institute (Contract 5085-260-1152) and by the National Science Foundation, Polymers Program, which provided computer time at the National Center for Supercomputing Applications, University of Illinois. Additional computations were performed at the John von Neumann Center, Princeton, with time provided by the JVNC National Allocation Committee.

## Appendix: Molecular Dynamics Procedure

The molecular dynamics procedure used is similar to that described previously in ref 2. A calculation of the time evolution of the system corresponding to give initial positions and velocities is performed, by the Verlet algorithm, for a period of time referred to as a block. A new set of initial velocities is then chosen, corresponding to a canonical ensemble at the prescribed temperature, and the process is repeated. A typical computation used 50 blocks, each with 5000 time steps. A time step $\Delta t = 0.1$ was used in units of $(m/\kappa)^{0.5}$.

Some modifications have been made in programming in order to take full advantage of the vector processors of supercomputers. The major change is for the portion of the code which computes noncovalent interactions and all related functions. In the previous computations, we used the near-neighbor table method and update this table every 10–20 time steps. For each atom, the near-neighbor table lists all atoms within a sphere centered at that atom. The radius of this sphere is determined by the cutoff distance $r_0$ of noncovalent interaction plus a distance which the atoms can travel between two consecutive updates of the near-neighbor table. The noncovalent interactions are calculated according to that table at each step. The codes have been vectorized for this method (ref 27). Since we have been working with a purely repulsive potential, the cutoff distance $r_0$ is relatively small and the number of near neighbors for each atom is relatively small too. Also, by symmetry, each pair interaction needs to be computed only once so that the average number of near neighbors in the computation can be reduced by a factor of 2. As a result we are dealing with short vectors (1–20 components) in the noncovalent interaction calculation. This reduces the efficiency of the program on supercomputers. To eliminate this problem, we change the near-neighbor table to an interaction-pair table which lists all atom pairs whose distance is smaller than the radius of the sphere defined above. This is done in almost the same way as for the near-neighbor table. At each time step, the atom positions are scattered into two long lists numbered sequentially according to the interaction-pair table. Most of the computations of noncovalent interaction can then be executed with this long vector, including all virial term calculations for the work presented here. Although the resultant noncovalent force on each atom is collected by a scalar code, this method still saves at least 30% of cpu time for our model systems. For a system of 500 atoms at reduced density 0.66, total cpu time for 250 000 steps, with an update of the interaction-pair table every 10 time steps, is approximately 2900 seconds on the Cray X-MP.

## References and Notes

(1) Gao, J.; Weiner, J. H. *Macromolecules* **1987**, *20*, 2520.
(2) Gao, J.; Weiner, J. H. *Macromolecules* **1987**, *20*, 2525.
(3) Gao, J.; Weiner, J. H. *Macromolecules* **1988**, *20*, 773.
(4) Note that the present value of the parameter $\epsilon/kT = 0.5$ is much larger than the value $\epsilon/kT = 0.05$ employed in ref 1–3. As a consequence, the spheres in the present calculations are much harder and $\sigma$ is a better measure of the effective hard-sphere diameter. For example, an interaction energy if $2kT$ is achieved at a separation distance of $0.92\sigma$.
(5) Swenson, R. J. *Am. J. Phys.* **1983**, *51*, 940. See also ref 1.
(6) See, for example: Ogden, R. W. *Rubber Chem. Technol.* **1986**, *59*, 361.
(7) Weiner, J. H.; Berman, D. H. *J. Chem. Phys.* **1985**, *82*, 548.
(8) Chandler, D.; Weeks, J. D.; Andersen, H. C. *Science (Washington, D.C.)* **1983**, *220*, 787.
(9) DiMarzio, E. A. *J. Chem. Phys.* **1962**, *36*, 1563.
(10) Tanaka, T.; Allen, G. *Macromolecules* **1977**, *10*, 426.
(11) Alder, B. J.; Wainwright, T. In *Transport Processes in Statistical Mechanics*; Prigogine, I., Ed.; Academic: New York, 1958. Ree, F. H.; Hoover, W. G. *J. Chem. Phys.* **1964**, *40*, 939.
(12) Ullman, R. *Macromolecules* **1986**, *19*, 1748.
(13) See, for example: Treloar, L. R. G. *The Physics of Rubber Elasticity*, 3rd ed.; Clarendon: Oxford, 1975; pp 125, 126.
(14) Ronca, G.; Allegra, G. *J. Chem. Phys.* **1975**, *63*, 4990.
(15) Flory, P. J. *Proc. R. Soc. London, A* **1976**, *351*, 351.
(16) Flory, P. J.; Erman, B. *Macromolecules* **1982**, *15*, 800.
(17) Erman, B.; Flory, P. J. *Macromolecules* **1982**, *15*, 806.
(18) Edwards, S. F. *Proc. Phys. Soc., London* **1967**, *92*, 9.
(19) DiMarzio, E. A. *Polym. Prepr. (Am. Chem. Soc., Div. Polym. Chem.)* **1968**, *9*, 256.
(20) de Gennes, P.-G. *J. Phys. Lett.* **1974**, *35*, L-133.
(21) Gaylord, R. J. *Polym. Eng. Sci.* **1979**, *19*, 263.
(22) Marucci, G. *Macromolecules* **1981**, *14*, 434.
(23) Gaylord, R. J.; Douglas, J. F. *Polym. Bull. (Berlin)*, in press.
(24) Doi, M.; Edward, S. F. *J. Chem. Soc., Faraday Trans. 2* **1978**, *74*, 1802.
(25) For a brief discussion (p 668) of the decrease in bond force with increase in density in a system of dimers with hard-sphere intermolecular interactions, see also: Honnell, K. G.; Hall, C. K.; Dickman, R. *J. Chem. Phys.* **1987**, *87*, 664.
(26) Berman, D.; Weiner, J. H. *J. Chem. Phys.* **1985**, *83*, 1311.
(27) Useful guides to vectorizable algorithms for molecular dynamics calculations: Rahman, A., unpublished lecture notes, Aug 2, 1985. Sullivan, F.; Mountain, R. D.; O'Connell, J. *J. Comput. Phys.* **1985**, *61*, 138.